A Predistortion Linearizer Using Envelope-Feedback Technique with Simplified Carrier Cancellation Scheme for Class-A and Class-AB Power Amplifiers

Hyun-Min Park, *Student Member, IEEE*, Dong-Hyun Baek, *Student Member, IEEE*, Kye-Ik Jeon, and Songcheol Hong, *Member, IEEE*

***Abstract*—A predistortion linearization method using an envelope-feedback technique is proposed and implemented in this paper. This linearizer compensates the gain and phase nonlinearity of power amplifier (PA) simultaneously by controlling both variable attenuator and phase shifter with the feedback of only the difference signal between input and output envelopes. A new carrier cancellation scheme composed of a minimization circuit, log detector, and vector modulator is also presented. This circuit achieves adaptive control of the linearizer by enabling direct measurement of out-of-band power. It is well suited to a multichannel system where the allocated channels are time variant. The principle of the proposed linearizer is described and simple AM–AM distortion analysis is presented analytically and graphically based on the conceptual schematic diagram. A two-tone test for a class-A PA at 1.855 GHz with frequency spacing of 1 MHz showed intermodulation-distortion reduction of maximum 16 dB and stable operation over 5-dB output power variation up to 4-dB backoff from the saturation power level. The proposed linearizer is also applicable to class-AB PA's without further special adjustments. The adaptation circuit is fully implemented with analog integrated circuits, which can further extend its applicability with the integration technology.**

***Index Terms*—AM–AM, AM–PM distortion, carrier cancellation, envelope feedback, linearization, power amplifier, predistortion.**

I. Introduction

PREDISTORTION linearization techniques can be roughly subdivided into data predistortion and signal predistortion [1]. Data predistortion techniques using digital signal processor (DSP) hardware are numerously reported [2]–[4]. However, these techniques are mostly used in conjunction with the transmitter system where designers must have an access to an unmodulated baseband signal, and may not be a cost-effective one for some applications. In the signal predistortion linearizers [5], a nonlinearity generator is inserted between the input signal and power amplifier (PA). The nonlinearity generator generally consists of active devices [6], which can be adjusted to produce intermodulation products that can cancel out those of the PA.

In this paper, we studied predistortion linearizer especially well suited to high-power amplifiers (HPA's) for repeater application, which performs RF signal predistortion on a time-domain base using the envelope-feedback technique. The principle of the linearizer can be best described by the third-order approximation of nonlinearity of the amplifier. To simplify the analysis, we present here an AM–AM conversion case by representing a bandpass RF signal in the general form

$$s(t) = e(t)\cos\left[\omega_c t + \phi(t)\right] \tag{1}$$

where $e(t)$ is the time-varying envelope and $\phi(t)$ is the time-varying phase of the RF signal.

The analysis is based on the conceptual schematic diagram, and describes how the circuit components operate to reduce distortions in the output envelope signal so that the resulting output RF signal has less of an out-of-band component. In Section II, we present a graphical result in a two-tone case, assuming perfect envelope detection and ideal vector modulator.

For the linearizers to be useful, they should guarantee stable operations regardless of circumstantial changes. To this end, we simplified the circuits of achieving carrier cancellation with the unique combination of a minimization circuit (MC), log detector, and vector modulator using only commercial analog integrated circuits (IC's) by adopting a simple *direct search algorithm*. The cancellation scheme proposed in this paper and described in Section III is well suited to a multichannel system where the positions of the currently used channel are not well defined. By direct measurement of out-of-band power with a log detector, stable carrier cancellation of over 50 dB was achieved. In Section IV, the complete linearizer circuit is described in detail. In Section V, we show measurement results of the implemented linearizer.

II. Principle of the Linearizer

To explain the principle of the linearizer, a two-tone signal case is depicted in Fig. 1. We assume that AM–AM and AM–PM conversions follow a similar curve [12], as is often true for class-A through class-AB and class-B PA's when the signal peak power level is sufficiently lower than the saturation level so that

Manuscript received October 11, 1999. This work was supported by the Korea Science and Engineering Foundation through the MINT Research Center, Dongguk University, under the Engineering Research Center Program.

H.-M. Park, D.-H. Baek, and S. Hong are with the Department of Electrical Engineering, Korea Advanced Institute of Science and Technology, Taejon 305-701, Korea (e-mail: hmpark@eeinfo.kaist.ac.kr).

K.-I. Jeon is with the LG Corporate Institute of Technology, Seoul 137-724, Korea.

Publisher Item Identifier S 0018-9480(00)05027-4.

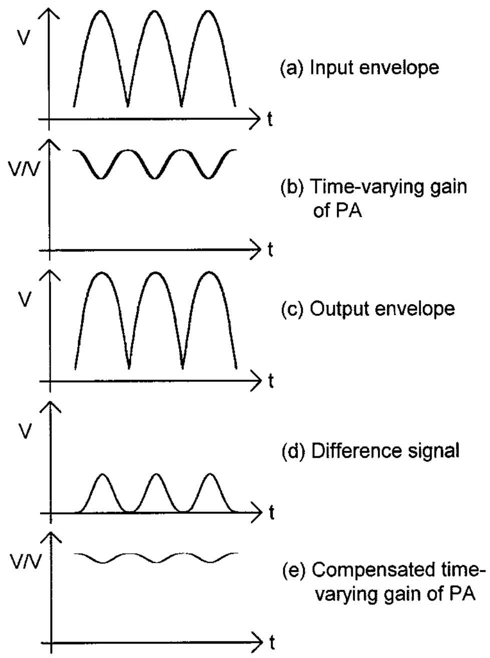

Fig. 1. Principle of the proposed linearizer.

the nonlinearities of PA's can be safely expressed by third-order polynomials. The AM–AM and AM–PM characteristics of the amplifier can be measured using CW single-tone signal [13]. For simplicity, we can look into only the AM–AM compensation through a variable attenuator. Since a two-tone signal has a time-varying envelope, it makes PA's operate in both linear and nonlinear regions so that gain characteristic of the PA shows time variance. As a result, the PA produces the top-compressed envelope at the output, as shown in Fig. 1(c). The difference signal between the input and output envelopes can be considered a measure of how much the PA distorts the input signal. It deviates from zero with the increase of the instantaneous power where it means that AM–AM conversion becomes significant. This implies that AM–AM conversion characteristics of the PA can be always obtained by extracting the difference signal when the input RF signal has a time-varying envelope. At this time, it is very important that the difference signal best describes the AM–AM conversion of the PA by the careful sampling of input and output RF signals. In the vicinity of a zero-crossing frequently occurred in the QPSK signal, the difference signal will shrink to zero. This means that the PA is operating in its linear region where it is not necessary to perform compensation. The gain function is, therefore, nearly constant for a brief period of zero crossing. The difference signal is fed back to control the variable attenuator in a way to compensate AM–AM conversion of the PA. The transfer characteristic of the variable attenuator changes according to its control signal, and the predistorted replica of the input RF signal is produced at the output of the variable attenuator. Thus, the overall gain of the system becomes more constant with the time variance of the input envelope. The same goes for AM–PM conversion of the PA with the phase shifter controlled by the same feedback signal.

Although it seems that the linearizer compensates AM–AM and AM–PM conversion by the variable attenuator and phase shifter separately, we actually achieve the simultaneous compensation by generating two feedback signals using the difference signal. As a result, two-dimensional compensation is achieved by using only scalar voltage quantity.

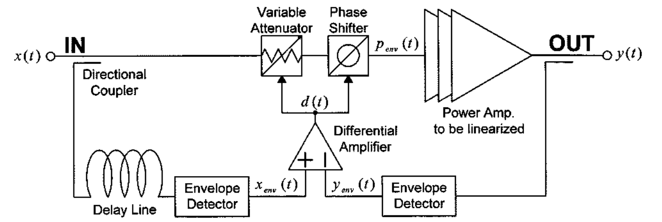

Fig. 2. Conceptual schematic diagram.

Fig. 2 shows the conceptual schematic diagram based on the above discussion. In a two-tone case with the same signal power, the input RF signal can be represented by

$$x(t) = 2A\cos\left(\frac{\Delta\omega}{2}t\right)\cos(\omega_c t) \tag{2}$$

where A is the amplitude of the individual signal, ω_c is the center frequency, and $\Delta\omega$ is the frequency spacing. If we assume that AM–AM conversion characteristics of the amplifier can be represented by the third-order polynomial and neglect AM–PM conversion to simplify the analysis, then the output signal before the activation of feedback loop is

$$\begin{aligned} y(t) &= a_1 x(t) + a_2 x^2(t) + a_3 x^3(t) \\ &= \frac{1}{2}a_2\left(2A\cos\frac{\Delta\omega}{2}t\right)^2 \\ &\quad + \left[a_1\left(2A\cos\frac{\Delta\omega}{2}t\right) + \frac{3}{4}a_3\left(2A\cos\frac{\Delta\omega}{2}t\right)^3\right] \\ &\quad \times \cos(\omega_c t) + \frac{1}{2}a_2\left(2A\cos\frac{\Delta\omega}{2}t\right)^2\cos(2\omega_c t) \\ &\quad + \frac{1}{4}a_3\left(2A\cos\frac{\Delta\omega}{2}t\right)^3\cos(3\omega_c t). \end{aligned} \tag{3}$$

Assuming an ideal bandpass coupler with full rejection of the out-of-band signal and perfect envelope detection, the envelope of $y(t)$ is

$$y_{\text{env}}(t) = a_1\left(2A\cos\frac{\Delta\omega}{2}t\right) + \frac{3}{4}a_3\left(2A\cos\frac{\Delta\omega}{2}t\right)^3. \tag{4}$$

After envelope detection, only the envelope term of the signal is sufficient to describe the principle of the linearizer. The difference signal generated is

$$\begin{aligned} d(t) = C_{\text{in}}\left(2A\cos\frac{\Delta\omega}{2}t\right) - C_{\text{out}}\Bigg[a_1\left(2A\cos\frac{\Delta\omega}{2}t\right) \\ + \frac{3}{4}a_3\left(2A\cos\frac{\Delta\omega}{2}t\right)^3\Bigg] \end{aligned} \tag{5}$$

where C_{in} and C_{out} represent the coupling ratio of the input and output coupler. By careful selection of C_{in} and C_{out}, we can make $d(t)$ describe the nonlinear characteristics of the amplifier as close as possible. The variable attenuator multiplies the input RF signal by $d(t)$. If we assume that the variable attenuator is linear at the vicinity of its operating point, it will produce at its output

$$p_{\mathrm{env}}(t) = \left(2A\,\cos\frac{\Delta\omega}{2}t\right)\left[\left\{C_{\mathrm{in}}\left(2A\,\cos\frac{\Delta\omega}{2}t\right) - C_{\mathrm{out}}\left(a_1\left(2A\,\cos\frac{\Delta\omega}{2}t\right) + \frac{3}{4}a_3\left(2A\,\cos\frac{\Delta\omega}{2}t\right)^3\right)\right\} \times g + 1\right] \tag{6}$$

where g is the slope of the transfer characteristic of the variable attenuator. When this predistorted signal is fed into the amplifier, the envelope of $y(t)$ would again be

$$y_{\mathrm{env}}(t) = a_1 p_{\mathrm{env}}(t) + \frac{3}{4}a_3 p_{\mathrm{env}}^3(t). \tag{7}$$

This completes one feedback cycle and, after several cycles, the feedback loop will be stabilized. Fig. 3 shows a normalized case based on (2)–(7) where $\Delta\omega$, A, C_{in}, and $C_{\mathrm{out}} = 1.0$ and $a_1 = 1.0$ and $a_3 = -0.03$. Fig. 3(a) shows linear input and nonlinear output envelopes and the corresponding difference signal. Fig. 3(b) shows linear and compensated envelopes. There is less distortion in the compensated envelope, which means the output RF signal has less of an out-of-band component.

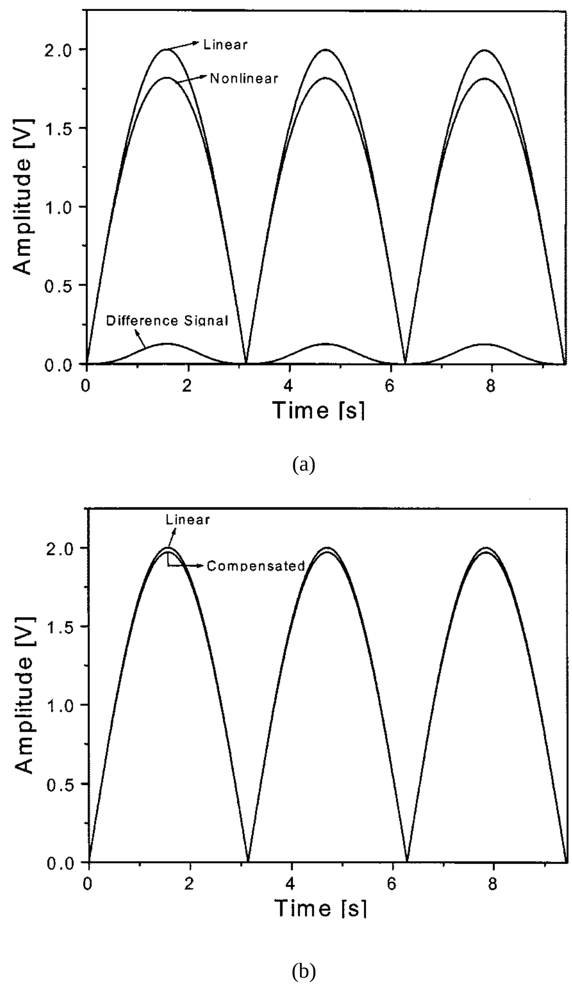

Fig. 3. Calculated signals in a normalized case. (a) Linear and nonlinear envelopes and difference signal. (b) Linear and compensated envelopes.

III. Carrier Cancellation Scheme

It is necessary to cancel the carrier signal to detect out-of-band power directly. Usually, the signal is downconverted to baseband where a bandpass filter (BPF) extracts out-of-band power. However, this will bring undesirable group-delay distortion or not be able to apply to a multichannel system where the allocated channels are not well defined.

To achieve cancellation between two signals along different paths, one signal is controlled to be 180° in phase and equal in amplitude of the other. The usual approach includes separate level detectors and phase detectors for different paths, but in this scheme, only one log detector is used, as shown in Fig. 4(a), since the level of the combined signal can be a direct measure of the degree of cancellation. This has additional benefits other than less involvement of components when the detector circuits for different paths suffer from the mismatch. Even when the signal is too weak or strong to be monitored by detectors, we can add only one auxiliary amplifier or attenuator to place the combined signal into the dynamic range of the log detector so that higher and more stable signal cancellation can be achieved. In this way, the proposed scheme does not suffer from any mismatch and requires less components.

The MC achieves the required adaptation. It utilizes a simple direct search technique and is described in Fig. 4(b). Each control signal for vector modulator is periodically moved up and down around its average value by a predetermined amount at several kilohertz, and the resultant signal levels are measured at the output of log detector. Two outcomes are separated by the single-pole double-throw (SPDT) switch, and the difference is extracted from the differential amplifier. The average value of control signal is modified in the integrator by comparing two outcomes until they become equal and the difference becomes zero. When this happens, further change in the control signal will have negligible effect on the level of the combined signal. Two identical blocks are merged into one MC for amplitude and phase control, respectively. By careful tuning of a predetermined value and frequency, we were able to achieve optimal cancellation of the carrier signal.

This carrier cancellation scheme also ensures that the characteristic of the signal path does not change with time. Since the signal path is composed of a vector modulator and PA whose composite transfer characteristic is time varying while the input and output signal samplers are mainly passive, the only possible condition for the consistent carrier cancellation is that the signal path becomes passive. As a result, the drifts of the PA are compensated. The entire circuit is implemented with commercial analog IC's rather than DSP's to avoid any programming so that, for further simplicity, it can be integrated with remaining

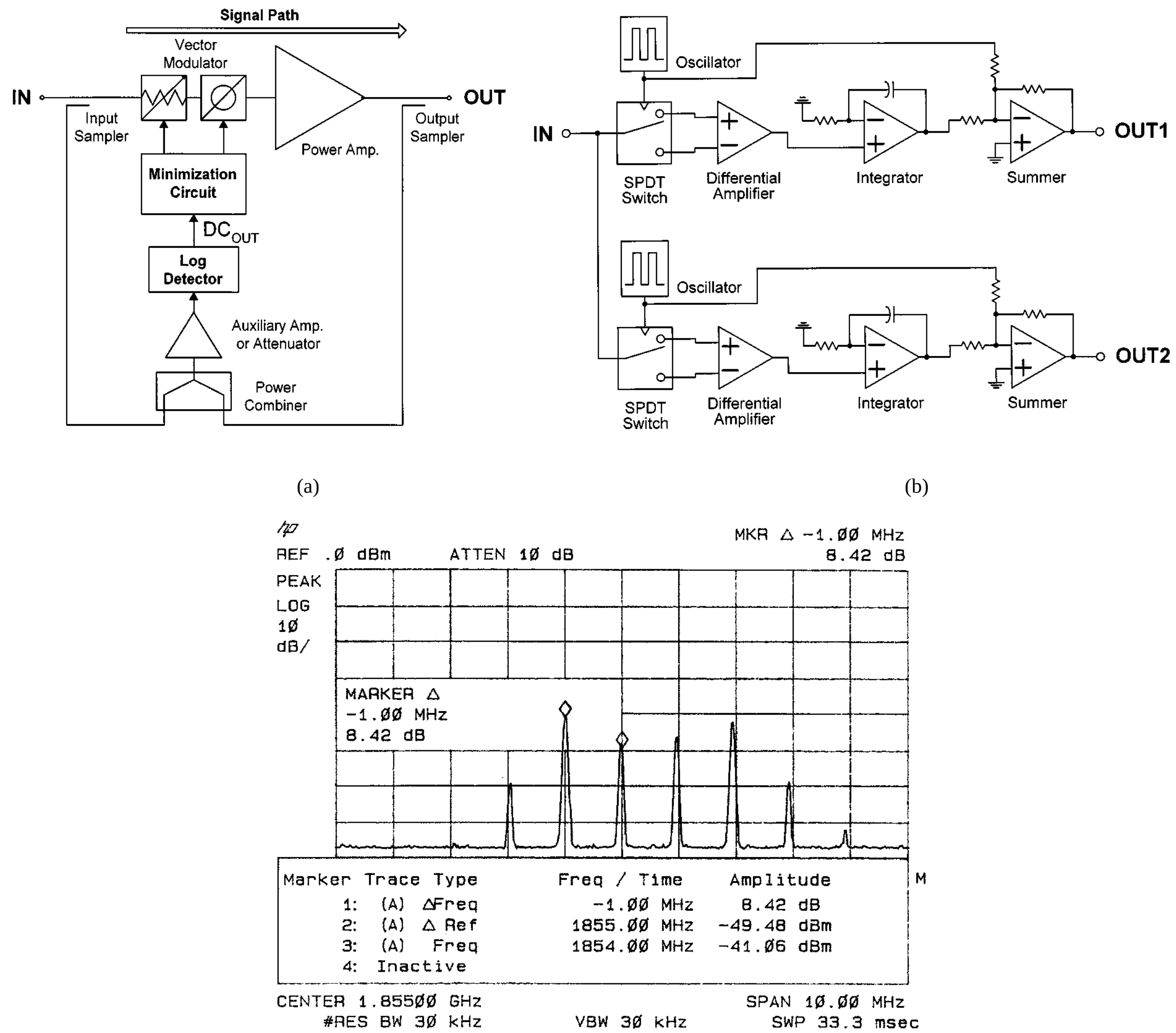

(a) (b) (c)

Fig. 4. (a) Proposed carrier cancellation scheme. (b) Schematic diagram of MC. (c) Measurement of carrier cancellation.

components. Fig. 4(c) shows the measurement result of the implemented carrier cancellation scheme. The signal is about 8 dB lower than IM_3, and this amounts to over 50-dB cancellation of the original signal.

IV. Implemented Linearizer

The complete circuit diagram is shown in Fig. 5. The input and output signals are sampled using a Wilkinson divider and the directional coupler, respectively. The envelopes of these signals are obtained using separate envelope detectors. They are fabricated with a Hewlett-Packard HSMS-2815, which contains a pair of Schottky diodes. It is very important to have sufficiently linear detectors not to add many distortions other than originated from the PA by a careful choice of the operating point of Schottky diodes used. The delay line before an input envelope detector is used to account for the time delay along the vector modulator and PA. The differential amplifier generates the difference signal. The feedback loop is divided into two separate ones for the amplitude and phase control, respectively. Each loop is composed of a variable gain amplifier (VGA) and a negative summer. Thus, the amplitude and bias of the final feedback signal can be varied independently for the optimal compensation to occur. Particularly, the IC's used in the feedback loop should operate fast enough as not to add much adverse time delay to the difference signal. Since the bandwidth (BW) of the difference signal is closely related to modulation BW of the input RF signal, the overall BW performance of the linearizer is critically dependent on these IC's. To meet the required BW specification, the IC's were selected on the basis of 3-dB BW, which was more than several tens of megahertz. This ensures that the difference signal best describes the nonlinear characteristic of the PA.

A variable attenuator and phase shifter are constructed from a 90° hybrid coupler, p-i-n diodes, and varactor diodes, respectively. Their response time should be at least more than ten times faster than the BW of the input RF signal as not to induce any time delay problem. The measured sensitivities to the control voltage were 1.8 dB/V and 5.4°/V. In the case of a variable attenuator, the maximum amount of gain compensation is below

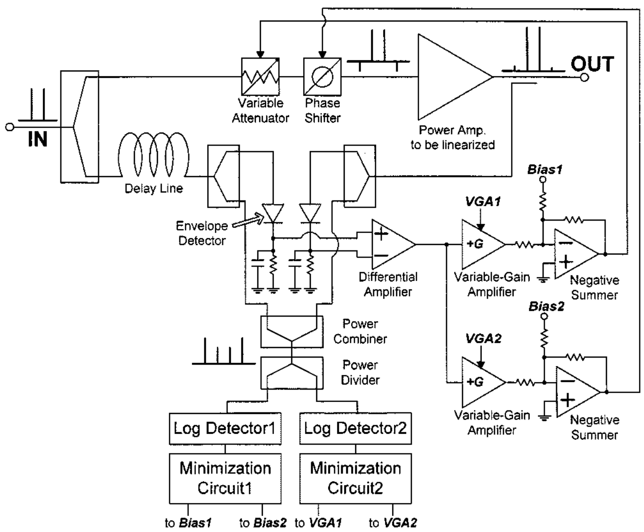

Fig. 5. Implemented circuit diagram.

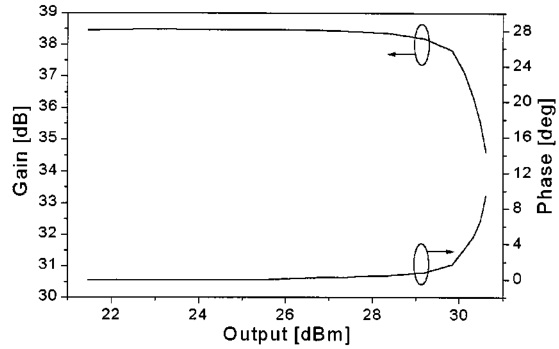

Fig. 6. Measured AM–AM and AM–PM conversions of a class-A PA (SNA586 + PA1074) at 1.855 GHz.

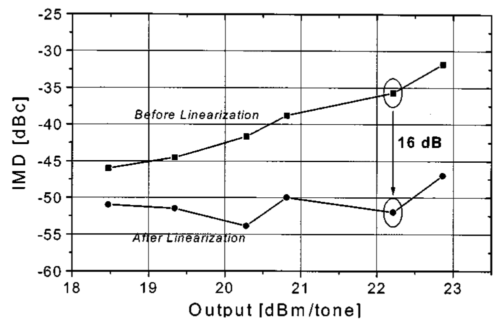

Fig. 7. Two-tone measurement of a class-A PA (SNA586 + PA1074) at 1.855 GHz with 1-MHz separation. The data were measured as the output power was varied.

several tenths of decibels. This is due to the fact that the operating average power of a PA is usually set at several decibels backoff from $P_{1\,\mathrm{dB}}$ and the instantaneous power does not exceed $P_{1\,\mathrm{dB}}$. Thus, the assumption that the attenuator is linear is valid under most circumstances.

Adaptive control of the linearizer is accomplished by two MC's. Our unique combination of the MC, log detector, and vector modulator simplifies the required adaptation into a conventional search for the minimum point of out-of-band signal power. Due to its close vicinity to carriers, Stapleton *et al.* [7] used a down-converter and BPF to extract it. In our scheme, MC_1 generates necessary bias voltages (*Bias1, Bias2*) for vector modulator based on the direct search algorithm [8], thus, by achieving carrier cancellation, the out-of-band signal power can be measured without using additional RF components. This has the added benefit of tracking drifts of PA's mainly caused by aging of transistors, temperature changes, switching between channels, and supply voltage variations since these characteristics do not require fast adaptation. By canceling out the carrier signal, only intermodulation products add to the output voltage of the log detector. In practice, many efforts have been exerted on the importance of carrier cancellation, which are essential in a feedforward system [9], [10].

The log detector circuitry was implemented using AD8313 (Analog Devices Inc., Norwood, MA) with a residual signal-strength indicator (RSSI) output. It was measured to have linear dynamic range of 60 dB. In our carrier cancellation scheme, a stable reduction of over 50 dB was achieved, which seems to be appropriate to be incorporated into predistortion linearizers where achieving IMD of over 50 dB is known to be difficult [11].

By direct monitoring of the out-of-band power made possible by carrier cancellation, MC_2 generates control voltages (*VGA1, VGA2*) to adjust the amplitudes of the feedback signals. Since the vector modulator can be assumed ideally linear in the vicinity of the operating point that has been optimized for carrier cancellation, it is possible to search for the minimum point of out-of-band power, as the amplitudes of the feedback signals are varied. By adding bias and difference signal in summers, it is possible to achieve carrier cancellation and RF predistortion within one vector modulator, which further simplifies implementation.

V. Measurement Results

To verify the applicability of the linearizer, we measured AM–AM and AM–PM conversions of a Class-A PA made up of an SNA-586 (Stanford Microdevices, Sunnyvale, CA) and PA1074 (Phoenix Microwave Corporation, Telford, PA), as shown in Fig. 6. In this figure, the similarity between AM–AM and AM–PM conversions as pointed out earlier in this paper are shown. A two-tone test at 1.855 GHz with frequency spacing of 1 MHz showed IMD reduction of maximum 16 dB and stable operation over 4.5-dB output power variation, as shown in Fig. 7. This implies the adaptation ability to PA drifts that were assumed to vary slowly with time. Fig. 8 shows the frequency spectrum results of a class-A PA with and without linearizer when the average output power is 26 dBm. An IMD reduction about 15 dB and a slight increase of higher order IMD products can be observed since they already showed sufficient linearity.

In Fig. 9, we showed measurement results under the same condition when the implemented linearizer was incorporated into a peak 60-W class-AB hybrid PA constructed from XRF282 and XRF284 (Motorola, Austin, TX). It showed IMD reduction of a maximum of 5 dB and stability over 6-dB output power variation. The amount of IMD reduction was smaller compared

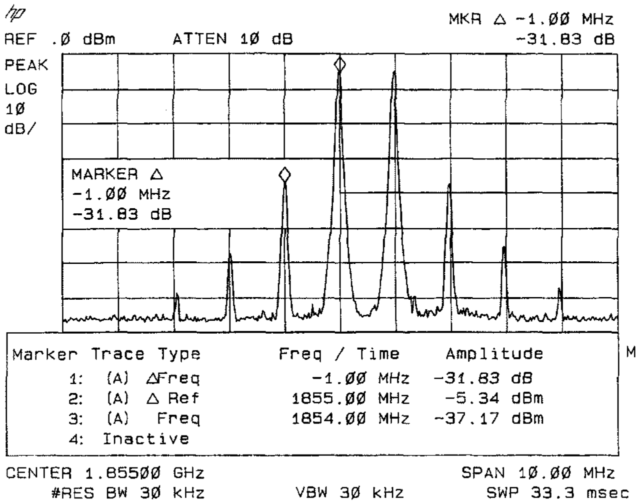

(a)

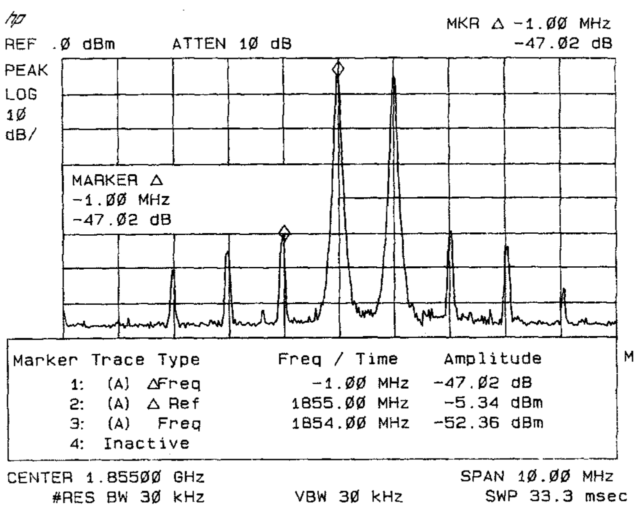

(b)

Fig. 8. Frequency spectrum of a class-A PA at 1.855 GHz with 1-MHz separation when average output power is 26 dBm. (a) Without linearizer. (b) With linearizer.

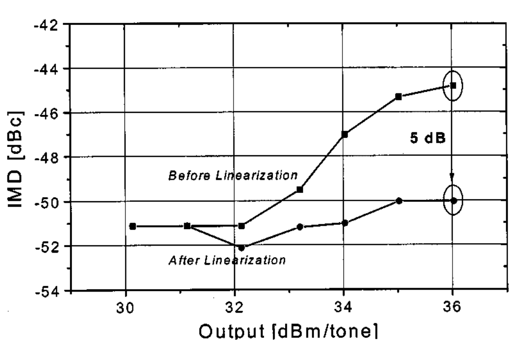

Fig. 9. Two-tone measurement of class-AB PA (60 W) at 1.855 GHz with 1-MHz separation. The data were measured as the output power was varied.

to that of class-A because measurement was done under more than a 9-dB output power backoff condition to find a relevant operating point of the PA considering peak-to-average ratio of the CDMA signal. It also showed IMD of no greater than 50 dBc, beyond which it is hard to achieve.

VI. Conclusion

In this paper, we proposed and implemented a predistortion linearization method using an envelope-feedback technique. We also proposed a new way to achieve carrier cancellation with the combination of an MC, log detector, and vector modulator to compensate slow drifts of PA's. This scheme simplifies the conventional approach and achieves stable cancellation of over 50 dB. The implemented linearizer was applicable to class-A and class-AB PA's and showed stable operation over output power variation, which means it can track the drifts of a PA adaptively. It is possible to eliminate the feedback loop and try open-loop control by using an input envelope rather than the difference signal if another way to achieve adaptation is provided. When the speed of convergence is important, a micro-controller can be incorporated to use a faster algorithm. Since the BW performance of the feedback linearizer is generally limited by the delay around the loop, it is recommended to integrate IC's into a single chip.

References

[1] A. N. D'Andrea, V. Lottici, and R. Reggiannini, "RF power amplifier linearization through amplitude and phase predistortion," *IEEE Trans. Commun.*, vol. 44, pp. 1477–1484, Nov. 1996.

[2] J. K. Cavers, "Amplifier linearization using a digital predistorter with fast adaptation and low memory requirements," *IEEE Trans. Veh. Technol.*, vol. 39, pp. 374–382, Nov. 1990.

[3] A. Bateman, R. J. Wilkinson, and J. D. Marvill, "The application of digital processing to transmitter linearization," in *8th European Electrotech. Conf.*, 1988, pp. 64–67.

[4] A. S. Wright and W. G. Durtler, "Experimental performance of an adaptive digital linearized power amplifier," *IEEE Trans. Veh. Technol.*, vol. 41, pp. 395–400, Nov. 1992.

[5] K. Yamauchi, K. Mori, M. Nakayama, Y. Mitsui, and T. Takagi, "A microwave miniaturized linearizer using a parallel diode with a bias feed resistance," *IEEE Trans. Microwave Theory Tech.*, vol. 45, pp. 2431–2435, Dec. 1997.

[6] R. C. Tupynamba and E. Camargo, "MESFET nonlinearities applied to predistortion linearizer design," in *IEEE MTT-S Int. Microwave Symp. Dig.*, 1992, pp. 955–958.

[7] S. P. Stapleton and F. C. Costescu, "An adaptive predistorter for a power amplifier based on adjacent channel emissions," *IEEE Trans. Veh. Technol.*, vol. 41, pp. 49–56, Feb. 1992.

[8] D. Wills, "A control system for a feedforward amplifier," *Microwave J.*, pp. 22–34, Apr. 1998.

[9] S. Kang, I. Lee, and K. Yoo, "Analysis and design of feedforward power amplifier," in *IEEE MTT-S Int. Microwave Symp. Dig.*, 1997, pp. 1519–1522.

[10] M. T. Hickson, D. K. Paul, P. Gardner, and K. Konstantinou, "High efficiency feedforward linearizers," in *Proc. 24th European Microwave Conf.*, 1994, pp. 819–824.

[11] A. Katz, "Linearizer basics," in *IEEE MTT-S Advances Amplifier Linearization Symp. Workshop*, Jun. 1998.

[12] C. G. Rey, "Adaptive polar work-function predistortion," *IEEE Trans. Microwave Theory Tech.*, vol. 47, pp. 722–726, Jun. 1999.

[13] C. Fallesen, G. Hanington, and P. M. Asbeck, "Improved linearity of a dynamic supply voltage power amplifier using digital predistortion," in *IEEE Power Amplifiers for Wireless Commun. Topical Workshop*, 1999, session 6.4.

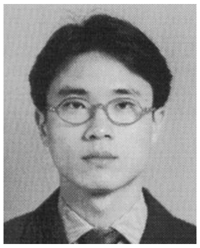

Hyun-Min Park (S'99) was born in Kwangju, Korea, in 1976. He received the B.S. and M.S. degrees in electrical engineering from the Korea Advanced Institute of Science and Technology (KAIST), Taejon, Korea, in 1997 and 1999, respectively, and is currently working toward the Ph.D. degree at KAIST.

His research interests include microwave PA and active device modeling and characterization.

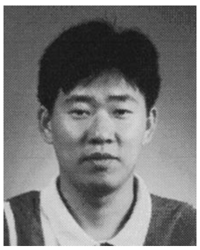

Dong-Hyun Baek (S'98) was born in Chechon, Korea, in 1973. He received the B.S. and M.S. degrees in electrical engineering from the Korea Advanced Institute of Science and Technology (KAIST), Taejon, Korea, in 1996 and 1998, respectively, and is currently working toward the Ph.D. degree at KAIST.

His research interests include high-PA's for wireless communication and quantum dot devices.

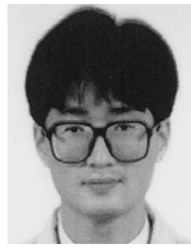

Kye-Ik Jeon was born in Korea, in 1968. He received the B.S., M.S., and Ph.D. degrees in electrical engineering from the Korea Advanced Institute of Science and Technology (KAIST), Taejon, Korea, in 1991, 1993, and 1998, respectively.

In April 1998, he joined the RF device team, LGCIT, Seoul, Korea. His research specialties are large-signal modeling of field-effect transistors (FET's) and heterojunction bipolar transistors (HBT's), linear power amplifiers (LPA's), monolithic-microwave integrated-circuit (MMIC) design, high-speed pulse measurements, and millimeter-wave module fabrications.

Songcheol Hong (S'87–M'88) was born in Korea, in 1959. He received the B.S. and M.S. degrees in electronics from the Seoul National University, Seoul, Korea, in 1982 and 1984, respectively, and the Ph.D. degree in electrical engineering from The University of Michigan at Ann Arbor, in 1989.

He is currently a Professor in the Department of Electrical Engineering, Korea Advanced Institute of Science and Technology (KAIST), Taejon, Korea. His research interests include optoelectronic IC's, quantum-effect devices, and MMIC's.